Journal of Pharmaceutics & Drug Development
Volume 10 | Issue 2
ISSN : 2348-9782

Research Article Open Access

# The Screening and Identification of Antibodies with Cross-Binding Activity to Human and Mouse IL-1R3

**Hui Qin[1,2,*], Xinrui Yu[2,3,*], Zhixin Yang[2], Jiao Liu[1,2], Gulisaina Qiaerxie[2,4], Jingmin Cui[2,4], Ye Tian[2], Xi Wang[2], Jinqiao Ma[2], Peng Du[2*] and Chunyang Zhou[1*]**

[1]North Sichuan Medical College, Nanchong 637000, Sichuan Province, China
[2]Beijing Institute of Biotechnology; Beijing 100071, China
[3]Hainan Medical University, Haikou 571158, Hainan Province, China
[4]Shenyang Pharmaceutical University, Shenyang 110000, Liaoning Province, China
[*]These authors contributed equally to this work.

[*]**Corresponding Author:** Chunyang Zhou, North Sichuan Medical College, Nanchong 637000, Sichuan Province, China. Tel: 1215486312, E-mail: zhouchunyang@nsmc.edu.cn

Peng Du, Beijing Institute of Biotechnology; Beijing 100071, China. E-mail: dependable@zju.edu.cn

**Citation:** Hui Qin, Xinrui Yu, Zhixin Yang, Jiao Liu, Chunyang Zhou, et al., (2023) The Screening and Identification of Antibodies with Cross- Binding Activity to Human and Mouse IL-1R3. J Pharma Drug Develop 10(2): 203.

**Received Date:** May 16, 2023 **Accepted Date:** June 16, 2023 **Published Date:** June 21, 2023

## Abstract

IL-1R3 is a common receptor for proinflammatory cytokines IL-1α, IL-1β, IL-33, IL-36α, IL-36β, and IL-36γ in the interleukin 1 family, and thus a potential therapeutic target for relevant diseases. In this study, we screen for and obtain antibodies with cross-binding activity to human and mouse IL-1R3 and explore the role of IL-1R3 pathway blockade in disease treatment. By alternately coating antibodies with human and murine IL-1R3, we identified five target antibodies from a phage-displayed human single-chain scFv) antibody library and preliminarily investigated their functional activity in vitro. We also improved the solubility of some antibodies by re-pairing light and heavy chains. By introducing antibodies AET1907 and 4H6L (by re-pairing antibody light and heavy chains) with comparable human-mouse cross-binding activity, our work lays the foundation for further scientific research and drug development.

**Keywords:** IL-1R3; antibody; phage-displayed antibody library; cross-binding activity; solubility

## Introduction

Inflammation arises through a complex network of dozens of molecules (including interleukin, interferon, chemo-kine, tumor necrosis factors, and acute-phase proteins) and many cell types (including monocytes, granulocytes, mast cells, and lymphocytes) [1-3]. Among the numerous cytokines involved in inflammation, the interleukin 1 (IL-1) family is involved in almost all types of inflammation and is an important inflammatory therapeutic target [1,2,4]. Interleukin 1 (IL-1) family members are central mediators of innate immunity and inflammation. In systemic or local pathological conditions such as tissue injury [5-7], autoimmune disease [8-11], infection [12,13], and tumors [14-16], IL-1 family members regulate the immune response of the body, including induction, maintenance, and amplification or antagonism of inflammatory signals. The IL-1 family consists of seven proinflammatory factors (IL-1α, IL-1β, IL-18, IL-33, IL-36α, IL-36β, and IL-36γ) and four anti-inflammatory factors or antagonists (IL-37, IL-38, IL-1Ra, and IL-36Ra) [17,18]. The IL-1 family of proinflammatory cytokines (e.g., IL-1, IL-18 and IL-33) plays a key role in the shaping and polarization of innate immunity and inflammatory response and is an important class of therapeutic targets [19-21]. IL-18 and IL-1primarily drive type I immune responses; IL-1 also drives Type III immune responses, and IL-33 is a driver of type II immune responses [17]. In addition, the IL-1 family has positive effects on the maintenance of homeostasis and mucosal immunity. A series of significant advances in the treatment of inflammatory diseases targeting members of the IL-1family have occurred recently. Kineret (Anakinra), a recombinant protein drug of IL-1RA, can effectively limit the activities of IL-1α and IL-1β and has been used in the treatment of rheumatoid arthritis (RA) [22] and in children and adults with early-onset multisystem inflammatory diseases (NOMID) [23]; in November 2022, the drug received emergency FDA approval to treat inflammation associated with SARS-CoV-2 infection [24-26]. Canakinumab (IIaris), which targets IL-1β, is approved for the treatment of autoimmune inflammatory diseases such as cold-pyrrolidine-related cyclical syndrome (CAPS) [27,28] and has the potential to reduce cardiovascular risk [29,30]. Spevigo (spesolimab), which targets IL-36R, was approved by the FDA (U.S. Food and Drug Administration) in 2022 for the treatment of generalized pustular psoriasis (GPP) [31,32], making it the only specific treatment for that disease.

Due to the heterogeneity and complexity of inflammatory diseases, a single condition is often associated with multiple IL-1 family members and their downstream proinflammatory factors. It has been reported that infections with coronaviruses, such as SARS--CoV-2, invade alveolar macrophages first to promote the secretion of massive inflammatory cytokines such as IL-1α, IL-33, and downstream IL-6. In mild cases, pathological changes such as pulmonary fibrosis occur; in severe cases, life-threatening hyper inflammatory reactions develop, eventually leading to acute respiratory distress syndrome[25,33]. In psoriasis, the abnormally high expressions of IL-1α and IL-36α are mutually reinforcing, accelerating the progression of autoimmune inflammation; in severe cases, the lesions worsen and even involve joints [34-36]. Therefore, satisfactory treatment may be difficult to achieve in certain diseases when using therapeutic strategies that target only a single proinflammatory factor in the IL-1 family.

Among the seven proinflammatory cytokines of the IL-1 family, IL-1α, IL-1β, IL-33, IL-36α, IL-36β, and IL-36γ share a common receptor component, the interleukin-1 receptor accessory protein (IL-1RAcP, also known as IL-1R3) [17,37,38]. IL-1R3 binds to IL-1R1, ST2, or IL-36R to form functional heterodimer complexes that mediate signal transduction of IL-1 [39], IL-33 [40], and IL-36, respectively [41,42]. Developing antibodies against IL-1R3 that block the functional activities of the six ligands, including IL-1, IL-33 and IL-36, may be more effective in regulating inflammation for complex inflammatory types involving multiple factors. In addition, such a strategy may lead to treatments that have broader applicability to disease types involving related factors. Therefore, IL-1R3 is a potential therapeutic target for inflammation-related diseases. In recent years, significant progress has been made in the research of antibody drugs targeting IL-1R3. Nadunolimab (CAN04), a humanized IgG1 monoclonal antibody (antibody-dependent cellular cytotoxicity (ADCC)-enhanced) developed by the Swedish company Cantargia AB, is targeted for the treatment of malignant tumors (non-small cell lung cancer). Phase I clinical results showed good safety and the treatment has now entered Phase II clinical studies [14,43,44]. Cantargia has also developed a second anti-IL1RAP antibody (CAN10) for the treatment of autoimmune diseases. In addition, German MAB Discovery has developed a humanized IgG1 monoclonal antibody MAB-16-0030 and modified its Fc fragement to reduce ADCC, which is still in the early stage of development. MAB Discovery uses a substitute antibody targeting IL-1R3 in mice model (MAB-16-0351), and in three mouse models (peritonitis induced by mono-

sodium urate crystal (MSU), allergic asthma induced by ovalbumin (OVA) and psoriasis induced by imiquimod) it has confirmed the positive role of IL-1R3 antibody in the treatment of broader inflammation [45]. Blockade of the functional activity of IL-1α, IL-1β, IL-33, IL-36α, IL-36β, and IL-36γ using antibodies that target IL1R3 may rapidly and effectively control the development of inflammation and the progression of related diseases [46].

Of note, no currently studied antibody targeting human IL-1R3 exists that can cross-bind with mouse IL-1R3, which makes the evaluation of the efficacy of the antibody in a mouse model in vivo difficult. Although IL-1R3-humanized mice can solve this problem to some extent, the use of humanized mice increases the cost of research. At the same time, IL-1R3 and its ligands are associated with various diseases and conditions, and the animal models for research are often complex. Many disease models may be difficult to construct using IL-1R3 humanized mice. More importantly, for antibodies that only bind to human IL-1R3, it is difficult to ensure the consistency of the mechanisms of action of the two antibodies when alternative antibodies are used for pharmaco dynamic evaluation in mouse models; this can result in dissonance between in vivo and in vitro outcomes. Therefore, the preparation of antibodies with cross-binding activity to both human and mouse IL-1R3 is helpful when studying the role of IL-1R3 and its ligands in diseases, and in developing valuable therapeutic drugs. In this study, we screened a phage antibody library by alternately coating potential antibodies with human and murine IL-1R3 and obtained five antibodies with cross-binding activities to human and mouse IL-1R3. One, AET1907, has similar affinity for human and mouse IL-1R3. We did preliminary studies on the functional activities of all five antibodies in vitro. In addition, we were able to improve the solubility of some antibodies by repairing antibody light and heavy chains. This study provides the foundation for subsequent mechanistic exploration and drug development.

## Materials and Methods

### Sequence and Structure Analysis

Protein sequence and structure alignments were done using Discovery Studio (Accelrys). The amino acid sequences of human and mouse IL-1R3 were acquired from Gen Bank (https://www.ncbi.nlm.nih.gov/genbank). The structures of these proteins were derived from PDB: 3O4O and PDB:5VI4, which are recorded in Protein Data Bank (http://www.rcsb.org). Molecular structure illustrations were generated using PyMOL Molecular Graphics Software or Discovery Studio. Screening and Identification of Phage-displayed Antibodies.

A phage-displayed human single-chain (scFv) antibody library with a high capacity of 1.35 × 1010 (maintained in our lab) was subject to multiple rounds of selection in Nunc-Immuno tubes (Nunc, Europe) coated with recombinant human IL-1R3 (Sino Biological, Beijing, China) or mouse IL-1R3 (Sino Biological, 52657-M08H, Beijing, China), in turn, and at decreasing concentrations. Several rounds of screening were done. In the first round of screening, the recombinant protein human IL-1R3 His was diluted with PBS to 20 μg/ml and added to the immunotube to coat it at 4 °C for 14-16 h. After being washed twice with PBS, the immunotube was blocked using a blocking buffer (2% bovine serum albumin (BSA; Sigma, St. Louis, MO) in PBS) at 37 °C for 1 h. The pre-blocked phage display antibody libraries were then added to the immunotube and incubated at 4 °C, 18 to 20 h. The next day the immunotube contents were discarded and the tube washed with PBST (PBS containing 0.1% Tween-20) 15 times and with PBS 10 times for 5 min per wash. Bound phages were eluted with 1ml of 0.1 M glycine-HCl (pH 2.2) and neutralized with 1 M Tris-HCl to pH 7.4. The neutralized eluate was collected and 9 mL of E. coli XL1-Blue in logarithmic growth phase was added to eluate and allowed to stand at room temperature for 30 min to allow infection. The culture was then transferred to a shaker at 37 °C and 150 rpm for 1 h. After amplification on 2 × YT -CTG medium (2 × YT medium containing 50 μg/ml chloramphenicol (C), 10 μg/ml tetracycline (T), and 1% glucose (G)) plates at 37 °C overnight, XL1-Blue cells were scraped and phages were rescued by the helper phage M13KO7 (MOI = 50). The culture supernatant was collected by centrifugation, 1/4 volume of PEG8000 Buffer (containing 20% PEG8000 and 2.5 M NaCl) was added, and the mixture placed on ice for at least 2 h. It was then centrifuged at 4 °C and 8000 rpm for 45 min, the supernatant discarded and the precipitate resuspended in 2-3 mL PBS containing 2% BSA. This was then fil-

tered through a 0.45 μm filter membrane for sterilization, and the titer measured. The selection protocols for the second to fifth rounds of screening were identical to that of the first round, except for the concentrations of coated antigen, the input phage particles and the wash strength (Table S1). Alternately, human IL-1R3-His at the concentration of 10 μg/ml was coated in the second round and mouse IL-1R3-His was coated in the last three round at decreasing concentrations of 3 μg/ml, 1.3 μg/ml, 1 μg/ml. In the last three round, when scraped to rescue phages, the collected bacterial liquid was used for picking monoclonals for preliminary identification simultaneously.

In the last three rounds of screening, single clones were screened by enzyme-linked immunosorbent assay (ELISA). A sterile 96-well plate was filled with 200 μl/well of 2 × YT-CTG medium and randomly selected monoclonal colonies were inoculated into the 96-well plate and cultured overnight at 37 °C and 220 rpm until saturated. The next day, 200 μl/well of 2 × YT-CT medium was added to a new sterile 96-well plate and 40 μl/well transferred from the old to the new 96-well plate. The saturated bacterial solution was cultured at 37 °C and 220 rpm for ~1.5 h to OD600 = 0.7. M13KO7 was added and the plate kept at room temperature for 45 min. Phage expression was induced by adding kanamycin and IPTG (Isopropyl β-D-thiogalactoside) at 30 °C and 200 rpm for 12 h, followed by centrifugation of 96-well plates at 4000 rpm for 10 min. Supernatants were collected in a new 96-well plate for ELISA identification. The 96-well plate (Corning, NY, USA) was coated with the positive antigen of human IL-1R3-His; BSA and KDR (Kinase Insert Domain Receptor, also known as VEGFR) with His tag were used as negative antigen controls. After blocking, phage particles blocked were added, and the plate was incubated at 37 °C for 1 h. Antigen recognitions were detected by 0.25 μg/ml horseradish peroxidase (HRP)–conjugated anti-M13 antibody (SinoBiological, Beijing, China), followed by the addition of Tetramethylbenzidine (TMB) buffer (Leikebio, LK-TMB-S-002, Bejing, China). Then, 2M H2SO4 was used to stop the reaction, and results were monitored at OD 450/595 nanometers (nm) with a microplate reader (Thermo Multiskin MK3). Positive clones were sequenced (MCZY Biotech, Beijing, China) to obtain target antibody genes.

## Preparation of Antibodies

Genes encoding variable regions of light or heavy chains of positive scFv antibodies were cloned into expression vectors pABL and pABG by double digestion of BsrG I and Hind III or Afl II and Nhe I (New England Biolabs, USA), respectively (both constructed in our lab). FreeStyle™ 293-F cells (Invitrogen, CA, USA) were co transfected with light and heavy chain vectors for simultaneous expression and cultured at 37 °C, 125 rpm and 5% CO2 for 4 days, then centrifuged at 8000 rpm for 10 min to collect the culture supernatant and filtered with 0.45 μm membrane for later use. Antibodies secreted in the supernatant were purified using HiTrap™ Mabselect SuRe™ (Cytiva, 11003493, USA), replacing 0.1 M Citric Acid Buffer (pH 3.0) with PBS (pH 7.4) using HiTrapTM desalting columns (Cytiva, 29048684, USA). A spectrophotometer (Thermo Nanodrop One C, NY, USA) was then used to quantify protein concentration, and the target protein was verified by 10% SDS-PAGE (Genscript, M00668, Nanjing, China).

## ELISA Assay

We coated 96-well microtiter plates (Costar, NY, USA) with recombinant human IL-1R3-His or mouse IL-1R3-His at a concentration of 1 μg/ml overnight at 4 °C. Plates were then blocked using phosphate-buffered saline (PBS) containing 2.5% fat-free powdered milk for 1 h at 37 °C. Purified antibodies were serially diluted (to 0.0565-10,000 ng/mL) in PBS buffer containing 2.5% fat-free powdered milk and 0.1% Tween 20 and then incubated for 1 h at 37 °C. And then add diluted antibody to ELISA plate, and combine with 96-well microtiter plates coated with blocked antigen for 1h at 37 °C. After washing, HRP-conjugated goat anti-human IgG (ZSGB-Bio, Beijing, China) was added, and the mixture incubated for 45 min at 37 °C, followed by the addition of TMB. Then, 2M H2SO4 was used to stop the reaction. The optical absorbance was measured at 450 nanometers (nm) with 595 nm as a reference (Thermo Multiskan MK3). Curves were plotted using Graph Pad Prism Software 9.0, using non-linear regression, and variable slope fifit, log (agonist) vs. Response - Variable slope to analyse the data.

### Surface Plasmon Resonance (SPR) Assay

The interaction affinity between antibodies and recombinant human IL-1R3 or mouse IL-1R3 was calculated from kinetic constants using the BIAcore™ T200 system. Multi-cycle kinetics was used for kinetic analysis experiments. Purified antibodies were captured on a protein A Sensor Chip (Cytiva, USA). Recombinant human IL-1R3 and mouse IL-1R3 with a concentration from 37.5-600 nanomolar (nM) in HBS-EP+ running buffer were passed over the chip at a rate of 30 μl/min at 25 °C. A 2-min association time was followed by a 2-min dissociation period. A cycle of repeated measurements was set for quality control, and two cycles of blank controls were used to correct for system deviations. The regeneration step consisted of chip flushing with 3 M MgCl2 for 30 s at the rate of 30 μl/min. The experimental data were fit to a 1:1 binding model using BIAcore™ T200 evaluation software.Equilibrium disassociation constants (KD) were calculated according to fitting curves.

### Cell Culture and Function Assay

A549 cells (human pulmonary carcinoma) preserved in our lab were cultured in high-glucose DMEM media (Procell, Wuhan, Beijing) supplemented with a 10% FBS (Tianhang Biotechnology Co., Ltd., Zhejiang, China) and a 1/100 penicillin-streptomycin solution (Procell, Wuhan, Beijing). HaCaT (human immortalized keratin-forming cells) cells were purchased from Procell Life Science & Technology Co., Ltd. and cultured in MEM media (Procell, Wuhan, Beijing) containing 10% FBS and 1/100 penicillin-streptomycin solution at 37 °C in a humidified 5% CO2 incubator. Cells were inoculated in 96-well plates (Costar, USA) to a final density of 1 × 104 cells/well and incubated with 20 μl of IL-IR3 antibodies or the standard for 3 h in the medium. Cells were then stimulated with IL-1β (working concentration = 40 g/ml) or IL-36α (working concentration = 25 ng/ml) for 24 h. Detection of IL-6 and IL-8 was performed by IL-6 ELISA kits (Elabscience, Wuhan, Beijing) and IL-8 ELISA kits (Elabscience, Wuhan, Beijing), respectively. The inhibition rate of antibodies was calculated by setting the OD at 450 nanometers (nm) with 595 nm as a reference in the absence of the antibodies (AET1907, AET1912) and human IL-1β (IL-36α) as 'Ao', in the presence of antibodies (AET1907, AET1912) and human IL-1β (IL-36α) at different concentration as 'As', and in the presence of human IL-1β (IL-36α) alone as 'Ab'. The inhibition rate of antibodies was calculated as:

### Re-pairing of Light and Heavy Chains of Antibodies

The light and heavy chains of five newly identified antibodies (AET1903, AET1904, AET1906, AET1907, and AET1912) were re--paired and co-transfected into HEK-293F cells. New antibody samples were obtained by expression and purification. The binding activities of the new antibodies to human and mouse IL-1R3 were assayed by ELISA. Antibody concentration-absorbance (OD) curves were plotted by GraphPad Prism Software 9.0, using non-linear regression, and variable slope fifit, log(agonist) vs. Response - Variable slope, and the half-maximal effective concentration (EC50) values calculated.

## Results

Alternating Screen by Human and Mouse IL-1R3 to Obtain Target Antibodies. Amino acid sequences of the extracellular domain of human and mouse IL-1R3 are >90% similar, with differences between sequences and structures observed in the ligand-binding region (Figure 1). Therefore, we alternately used human and mouse IL-1R3 for panning in a human single-chain antibody (scFv) phage display library (Table S1). A variety of phage antibodies with specific binding activity to human IL-1R3 were obtained (Figure 2A). According to sequencing, five antibody variable domain genes were enriched. Genes encoding the light and heavy chains of these five antibodies were cloned into expression vectors pABL (λ light chain) and pABG (γ1 heavy chain), respectively (Figure S1). Then, paired light and heavy chain plasmids were co-transfected into HEK-293F cells for expression. These five IgG1λ antibodies, named AET1903, AET1904, AET1906, AET1907 and AET1912, were obtained by affinity purification (Figure S2). The candidate antibody was evaluated by Tm & Tagg with optional DLS procedure, all antibodies showed good stability (Table S2) and with Tm values all above 60 °C, the five candidate antibodies had good thermal stability. Binding specificity was approximated using ELISA and all five antibodies were able to effectively bind to both human and mouse IL-1R3 without cross-reactivity to nega-

tive control antigens (Figure 2B).

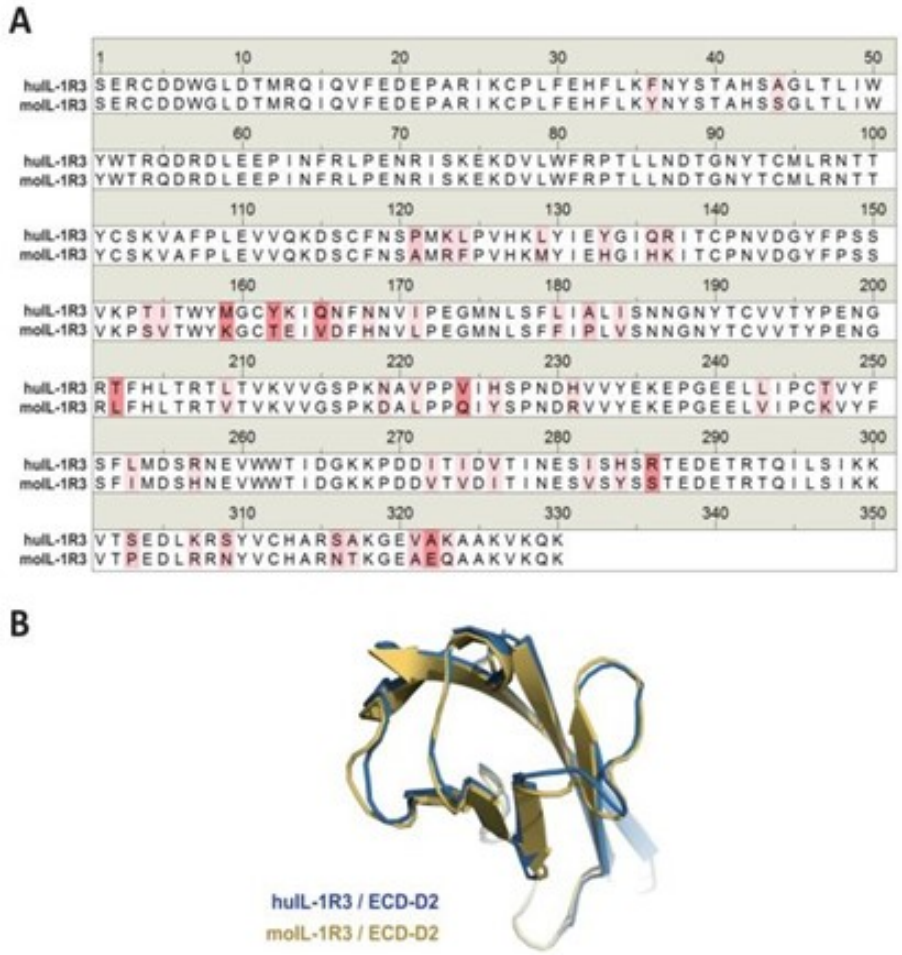


**Figure1:** Sequence and structure analysis of human IL-1R3 (huIL-1R3) and mouse IL-1R3 (moIL-1R3). (A) Sequence alignment of human and mouse IL-1R3. The amino acid similarity was shaded differently. (B) Structure alignment of extracellular domain D2 (ECD-D2, 120-215AA as shown in (A)) of human and mouse IL-1R3, which covers its most ligand recognition region.

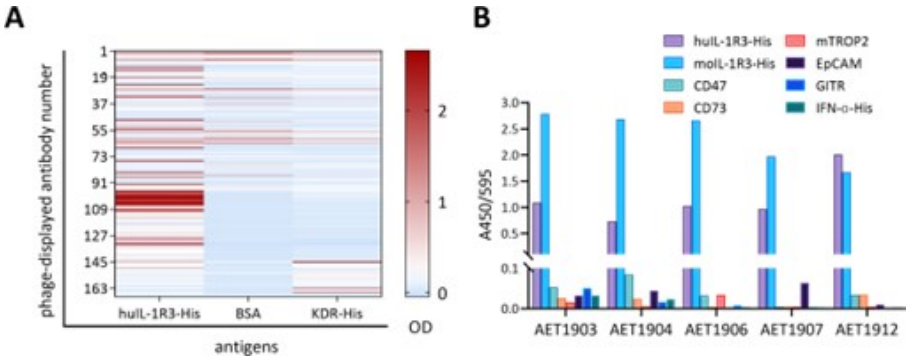


**Figure2:** Identification of phage-displayed antibodies selected from the library (A) and binding specificity of enriched antibodies (B). (A) Recombinant human IL-1R3 with histidine tag (huIL-1R3-His) and negative antigen controls (BSA and KDR-His) were parallelly coated in an ELISA assay and the optical density (OD) measured. (B) The binding specificity was approximated using ELISA. The coating amount of human IL-1R3 (huIL-1R3-His) and mouse IL-1R3 (moIL-1R3-His) was 50 ng/well, while that of other antigens was 100 ng/well. The concentration of antibody was 10 μg/ml.

## Affinity of Antibodies

The interactions between serially diluted antibodies and human IL-1R3 or mouse IL-1R3 were also detected by ELISA. All antibodies had favorable binding activity to both human and mouse IL-1R3 in a dose-dependent manner (Figure 3). Among them, AET1912 exhibited the highest binding activity to human IL-1R3. All antibodies except for AET1912 showed similar binding activity to mouse IL-1R3. We further examined the affinity of antibodies through surface plasmon resonance (SPR) analysis using the BIAcore™ T200 system. Representative sensorgrams are presented in Figure 4 and the kinetic parameters are shown in Table 1. AET1907 and AET1912 displayed favorable responses to both human and mouse IL-1R3 and AET1907 shared comparable affinity to human and mouse IL-1R3.

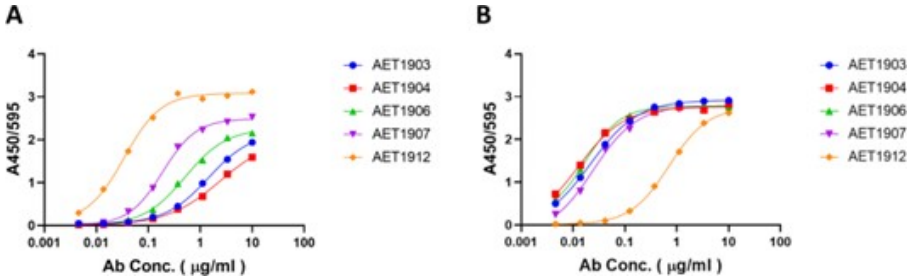


**Figure3:** The binding activity of antibodies to (A) human IL-1R3 and (B) mouse IL-1R3. Human or mouse IL-1R3 were coated in 96-well microtiter plates at 100 ng/well and serially diluted antibodies were detected by ELISA assay.

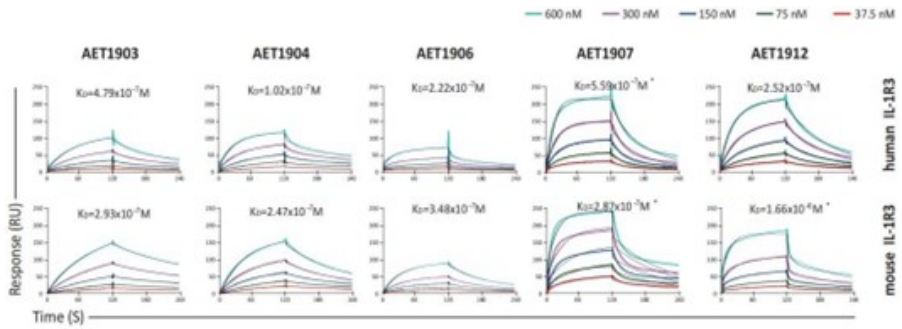


**Figure4:** Representative sensorgrams of antibodies in SPR assays. The antibodies were immobilized separately on the sensor chip surface, and human and mouse IL-1R3-His at serially diluted (37.5-600 nM) concentrations were passed over the chip. The fitting curves (thin black lines) were derived from analysis using the 1:1 binding mode. Equilibrium disassociation constants (KD) were calculated according to fitting curves.

**Table1:** Affinity constant of antibodies interacting with human and mouse IL-1R3

| Anti body | Antigen | ka (104M-1s-1) | kd (10-3s-1) | KD (10-7M) | $\chi 2$ (RU²) |
|---|---|---|---|---|---|
| AET1903 | huIL-1R3 | 1.76 | 8.44 | 4.79 | 6.72 |
| | moIL-1R3 | 1.63 | 4.76 | 2.93 | 3.25 |
| AET1904 | huIL-1R3 | 8.68 | 8.81 | 1.02 | 5.72 |
| | moIL-1R3 | 4.11 | 10.12 | 2.47 | 2.89 |
| AET1906 | huIL-1R3 | 4.01 | 8.89 | 2.22 | 6.83 |
| | moIL-1R3 | 3.15 | 10.9 | 3.48 | 0.82 |
| AET1907 | huIL-1R3 | - | - | 5.59* | 1.35 |
| | moIL-1R3 | - | - | 2.87* | 0.84 |
| AET1912 | huIL-1R3 | 4.61 | 11.6 | 2.52 | 9.91 |
| | moIL-1R3 | - | - | 16.6* | 1.77 |

ka, association rate constant; kd, disassociation rate constant; KD, equilibrium disassociation constant; KD=kd/ka. $\chi 2$ is the chi-square value between the fitting curves and response curves. *The value is derived from the steady-state calculation (1:1 binding) for a better fit. Antibodies Effectively Blocked IL-1R3-Mediated Activities Ex Vivo. To determine the blocking function of the IL-1R3 antibodies to IL-1R3-associated ligand signaling, we used IL-1β stimulation of A549 cells to measure release of IL-6 and used IL-36α stimulation of HaCaT cells to detect secretion of IL-8 (Figure S3). In our study, purified AET1903, AET1904, and AET1906 exhibited insufficient solubility in PBS for functional assays. Therefore, the ex vivo activity assay proceeded using only AET1907 and AET1912. In A549 cells, the two antibodies significantly inhibited IL-6 production in a dose-dependent manner; antibodies at the highest concentration (1 mg/mL) decreased cytokine production significantly, by 82.09% (AET1907) and 87.05% (AET1912) (Figure 5A, B). In HaCaT cells, the two antibodies also significantly inhibited IL-8 production; at 1.5 mg/mL antibodies decreased cytokine production significantly by 60.9% (AET1907) and 79.5% (AET1912) (Figure 5C D). Thus, both AET1907 and AET1912 seem to recognize a proper epitope on the IL-1R3 surface that overlapped the ligands' binding region to some extent and interfered with IL-1R3-mediated downstream signaling.

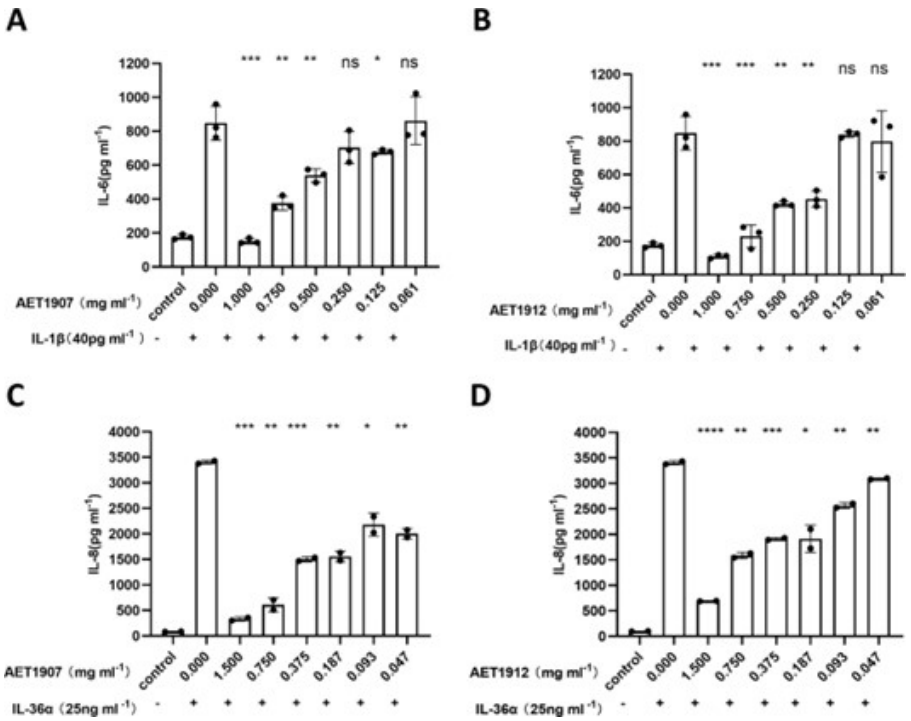


**Figure5:** Antibodies effectively blocked IL-1R3-mediated functional activity. (A, B) Inhibitory effects of (A) AET1907 and (B) AET1912 on IL-1β-stimulated IL-6 secretion of human lung epithelial cell line (A549). (C, D) Inhibitory effects of (C) AET1907 and (D) AET1912 on IL-36α-stimulated IL-8 secretion of human keratinocyte cell line (HaCaT). Data were processed using Graph Pad Prism Software, and data shown are mean ± SD from one representative experiment. ****p-value <0.0001, ***p-value <0.001, **p-value <0.01, *p-value <0.05 (unpaired t-test). (A)(B), n = 3; (C) (D), n = 2.

## Re-pairing of Antibodies and Identification

Despite their low solubility, AET1903, AET1904, and AET1906 displayed a gentler disassociation phase compared to AET1907 and AET1912 when interacting with mouse IL-1R3 (Figure 4). In addition, the five antibodies were selected from the same library, and their variable regions share similar framework (FR) amino acid sequences. Therefore, we attempted to re-pair the light and heavy chains of the five antibodies in the hope of obtaining antibodies with improved solubility and affinity. The binding activities of newly paired antibodies were estimated (Table S3). Unfortunately, we did not obtain new antibodies with significantly improved binding activity to human and mouse IL-1R3. Only one repairing, 4H6L displayed slightly improved affinity but apparently favorable kinetics curves compared with AET1904 and AET1906 (Figure S5 and Table S4). 4H6L also shared comparable affini-

ty to human and mouse IL-1R3. More importantly, 4H6L exhibited remarkably improved solubility in PBS (pH 7.4), exceeding 10 mg/ml (in comparison, saturated precipitation for AET1904 and AET1906 occurred at concentrations above 3 mg/ml at 4 °C (Figure S4) and saturated concentrations of AET1904 and AET1906 were <2 mg/ml). Our results suggest that re-pairing heavy and light chains may be helpful to improve antibodies' physicochemical properties, e.g., solubility.

## Discussion

Pro inflammatory cytokines of the IL-1 family are closely related to the occurrence and development of various inflammatory diseases. At the same time, it is also necessary to fully realize that due to the heterogeneity and complexity of inflammatory diseases (especially the excessive inflammation caused by severe infection and autoimmune diseases such as psoriasis and asthma), a single disease is often associated with multiple IL-1 family members and their downstream pro-inflammatory factors. As a result, a therapeutic strategy targeting a single factor may rarely achieve a good treatment effect. As a receptor common to many pro-inflammatory cytokines of the IL-1 family, IL-1R3 is a potential antibody drug target for the treatment of complex inflammatory-related diseases. Considering the complexity of experimental animal models of inflammatory diseases, the discovery of functional antibody molecules with binding activity to both human and mouse IL-1R3 can facilitate studies of mechanisms and drug development. To date, investigational IL-1R3 antibody drugs featuring human and mouse cross-binding activity have been scarce. Based on the sequence and structure analysis of human and mouse IL-1R3 (Figure 1) and panning of a phage-displayed antibody library alternatively coated with human and mouse IL-1R3 (Table S1), we successfully obtained novel antibodies with cross-binding activity to human and mouse IL-1R3 (Figure 3). All antibodies showed good stability (Table S2) and were able to effectively bind to both human IL-1R3 and mouse IL-1R3 without cross-reactivity to negative control antigens (Figure 2B). A similar strategy has also been reported in our previous work [47]. Therefore, this strategy may be serviceable for antibody discovery where a specific need must be met. Among these antibodies, AET1907 has comparable affinity to human and murine IL-1R3 and similar kinetic profiles for the interaction (Figure 4, Table 1). Additionally, AET1907 showed favorable specificity and could effectively inhibit IL-1R3-mediated secretion of cyto-Kines. We have further made efforts to obtain a series of new antibodies by re-pairing the light and heavy chains of the five discovered antibodies, from which we created the antibody 4H6L with improved kinetics curves, comparable affinity to human and mouse IL-1R3 (Figure S5 and Table S4), and increased solubility compared to AET1906 (Figure S4). This finding resulted in another favorable antibody molecule for our research and provides a strategy to improve molecular physicochemical properties (e.g., solubility) in the molecular discovery stage. Although the antibodies obtained so far do not display sufficiently high affinity to human or mouse IL-1R3 for clinical application, we anticipate being able to optimize the antibodies, especially AET1907 and 4H6L which share a similar affinity to human and mouse IL-1R3, in future work and to develop drug candidates for inflammatory diseases.

## Conclusion

In our study, we focused on screening antibodies with human-mouse cross-binding activity at the molecular discovery stage, and successfully obtained a favorable candidate molecule AET1907. By re-pairing the light and heavy chains of all five discovered antibodies, we obtained a new candidate antibody 4H6L with improved characteristics (in this case, solubility). The affinity of the two antibodies to human IL-1R3 and mouse IL-1R3 is equivalent, and the two antibodies have the potential to be developed into antibody medicines after further optimization and modification.

## Author Contributions

Conceptualization, H.Q., X.Y. and Z.Y.; methodology, H.Q., J.M. and X.Y.; software, H.Q. and J.C.; validation, H.Q. and Z.Y.; resources, H.Q., X.Y. and G.Q.; data curation, H.Q., X.W. and Y.T.; project administration, C.Z. and P.D.; writing-original draft preparation, H.Q., X.Y. and P.D.; writing-review and editing, H.Q. and P.D.; visualization, H.Q. and J.L.; supervision, P.D., C.Z. and

Z.Y. All authors have read and agreed to the published version of the manuscript.

## Funding

This research received no external funding.

## Institutional Review Board Statement

Not applicable.

## Informed Consent Statement

Not applicable.

## Data Availability Statement

Data are available from the authors upon reasonable request.

## Acknowledgments

Thanks are extended to Dr. Guanying Zhang (Beijing Institute of Biotechnology) for technical and equipment support.

## Conflicts of Interest

The authors report no competing interests to declare.

## References

1. Medzhitov R (2021) The spectrum of inflammatory responses. Science 374: 1070-5.

2. Fajgenbaum DC, June CH, Cytokine Storm (2020) 383: 2255-73.

3. Chen L, Deng H, Cui H, Fang J, Zuo Z, et al., (2018) Inflammatory responses and inflammation associated diseases in organs. Oncotarget 9: 7204-18.

4. Korbecki J, Bajdak-Rusinek K (2019) The effect of palmitic acid on inflammatory response in macrophages: an overview of molecular mechanisms. Inflamm Res 68: 915-932.

5. Bretheau F, Castellanos-Molina A, Belanger D, Kusik M, Mailhot B, et al., (2022) The alarmin interleukin-1alpha triggers secondary degeneration through reactive astrocytes and endothelium after spinal cord injury. Nat Commun 13: 5786.

6. Janko M, Ontiveros F, Fitzgerald TJ, Deng A, DeCicco M, et al., (2012) IL-1 generated subsequent to radiation-induced tissue injury contributes to the pathogenesis of radiodermatitis. Radiat Res 178: 166-172.

7. Martin SJ, Frezza V, Davidovich P, Najda Z, Clancy (2022) D.M. IL-1 family cytokines serve as 'activity recognition receptors' for aberrant protease activity indicative of danger. Cytokine 157: 155935.

8. Siebert S, Tsoukas A, Robertson J, McInnes I (2015) Cytokines as therapeutic targets in rheumatoid arthritis and other inflammatory diseases. Pharmacol Rev 67: 280-309.

9. Dinarello CA (2019) The IL-1 family of cytokines and receptors in rheumatic diseases. Nat Rev Rheumatol 15: 612-632.

10. Xie L, Huang Z, Li H, Liu X, Zheng S, et al., (2019) W. IL-38: A New Player in Inflammatory Autoimmune Disorders. Biomolecules.

11. Shakerian L, Kolahdooz H, Garousi M, Keyvani V, Kamal Kheder R, (2022) IL-33/ST2 axis in autoimmune disease. Cytokine 2022, 158: 156015.

12. Xu L, Wei C, Chen Y, Wu Y, Shou X, et al., (2022) IL-33 induces thymic involution- associated naive T cell aging and impairs host control of severe infection. Nat Commun 13: 6881.

13. Declercq J, De Leeuw E, Lambrecht BN, (2022) Inflammasomes and IL-1 family cytokines in SARS-CoV-2 infection: from prognostic marker to therapeutic agent. Cytokine 157: 155934,

14. Robbrecht D, Jungels C, Sorensen MM, Spanggaard I, Eskens F, et al., First-in-human phase 1 dose-escalation study of CAN04, a first-in-class interleukin-1 receptor accessory protein (IL1RAP) antibody in patients with solid tumours 126: 1010-7.

15. Zhang W, Borcherding N, Kolb R (2020) IL-1 Signaling in Tumor Microenvironment 1240: 1-23.

16. Liu Y, Gao Y, Lin T (2021) Expression of interleukin-1 (IL-1), IL-6, and tumor necrosis factor-alpha (TNF-alpha) in non-small cell lung cancer and its relationship with the occurrence and prognosis of cancer pain. Ann Palliat Med 10: 12759-66.

17. Mantovani A, Dinarello CA, Molgora M, Garlanda C (2019) Interleukin-1 and Related Cytokines in the Regulation of Inflammation and Immunity. Immunity 50: 778-95.

18. Migliorini P, Italiani P, Pratesi F, Puxeddu I, Boraschi D (2020) The IL-1 family cytokines and receptors in autoimmune diseases. Autoimmun Rev 19: 102617.

19. Palomo J, Dietrich D, Martin P, Palmer G, Gabay C (2015) The interleukin (IL)-1 cytokine family--Balance between agonists and antagonists in inflammatory diseases. Cytokine 76: 25-37.

20. Van Den Eeckhout B, Tavernier J, Gerlo S (2020) Interleukin-1 as Innate Mediator of T Cell Immunity. Front Immunol 2020, 11: 621931.

21. Dinarello CA (2009) Immunological and inflammatory functions of the interleukin-1 family. Annu Rev Immunol 27: 519-50.

22. Bedaiwi MK, Almaghlouth I, Omair MA (2021) Effectiveness and adverse effects of anakinra in treatment of rheumatoid arthritis: a systematic review. Eur Rev Med Pharmacol Sci 25: 7833-9

23. Kim YH, Kim BJ, Han J, Choi BY, Lee S (2021) Long-Term Efficacy of Anakinra in Cryopyrin-Associated Periodic Syndrome:

24. ocus on Destructive Arthropathy. J Clin Immunol 41: 1936-9

25. Elmekaty EZI, Maklad A, Abouelhassan R, Munir W, Ibrahim MIM, et al., (2023) Evaluation of anakinra in the management of patients with COVID-19 infection: A randomized clinical trial. Front Microbiol 14: 1098703

26. group (2021) C.-C. Effect of anakinra versus usual care in adults in hospital with COVID-19 and mild-to-moderate pneumonia (CORIMUNO-ANA-1): a randomised controlled trial. Lancet Respir Med 9: 295-304.

27. Bertoni A, Penco F, Mollica H, Bocca P, Prigione I et al., (2022) Spontaneous NLRP3 inflammasome-driven IL-1-beta secretion is induced in severe COVID-19 patients and responds to anakinra treatment. J Allergy Clin Immunol 150: 796-805.

28. Torene R, Nirmala N, Obici L, Cattalini M, Tormey V et al., (2017) Canakinumab reverses overexpression of inflammatory response genes in tumour necrosis factor receptor-associated periodic syndrome. Ann Rheum Dis 76: 303-9.

29. Yokota S, Kikuchi M, Nozawa T, Kizawa T, Kanetaka T et al., (2012) [An approach to the patients with cryopyrin-associated periodic syndrome (CAPS): a new biologic response modifier, canakinumab]. Nihon Rinsho Meneki Gakkai Kaishi 35: 23-9.

30. Ortega-Paz L, Capodanno D, Angiolillo DJ (2021) Canakinumab for secondary prevention of coronary artery disease. Future Car Diol 17: 427-42.

31. Dhorepatil A, Ball S, Ghosh RK, Kondapaneni M, Lavie CJ (2019) Canakinumab: Promises and Future in Cardiometabolic Diseases and Malignancy. Am J Med 132: 312-24.

32. Ali F, Smith CH, Mahil SK (2023) Spesolimab in the treatment of generalized pustular psoriasis: a critically appraised research paper. Br J Dermatol 188: 328-9.

33. Navarini AA, Prinz JC, Morita A, Tsai TF, Viguier MA, et al., (2022) Spesolimab improves patient-reported outcomes in patients with generalized pustular psoriasis: Results from the Effisayil 1 study. J Eur Acad Dermatol Venereol.

34. Makaremi S, Asgarzadeh A, Kianfar H, Mohammadnia A, Asghariazar V, et al., (2022) The role of IL-1 family of cyto- kines and receptors in pathogenesis of COVID-19. Inflamm Res 71: 923-47.

35. Gresnigt MS, van de Veerdonk FL (2013) Biology of IL-36 cytokines and their role in disease. Semin Immunol 25: 458-65.

36. Milora KA, Fu H, Dubaz O, Jensen LE (2015) Unprocessed Interleukin-36alpha Regulates Psoriasis-Like Skin Inflammation in Cooperation With Interleukin-1. J Invest Dermatol 135: 2992-3000

37. Calabrese L, Fiocco Z, Satoh TK, Peris K, French LE (2022) Therapeutic potential of targeting interleukin-1 family cytokines in chronic inflammatory skin diseases. Br J Dermatol 186: 925-41.

38. Boraschi D, Italiani P, Weil S, Martin MU (2018) The family of the interleukin-1 receptors. Immunol Rev 281: 197-232.

39. Jensen LE (2017) Interleukin-36 cytokines may overcome microbial immune evasion strategies that inhibit interleukin-1 family signaling. Sci Signal 10

40. Dinarello CA (2011) Interleukin-1 in the pathogenesis and treatment of inflammatory diseases. Blood 117: 3720-32.

41. De Martinis M, Ginaldi L, Sirufo MM, Bassino EM, De Pietro F, et al., (2020) IL-33/Vitamin D Crosstalk in Psoriasis-Associated Osteoporosis. Front Immunol 11: 604055.

42. Sullivan GP, Henry CM, Clancy DM, Mametnabiev T, Belotcerkovskaya E, et al., (2018) Suppressing IL-36-driven inflammation using peptide pseudosubstrates for neutrophil proteases. Cell Death 9: 378.

43. Broderick L, Hoffman HM (2022) IL-1 and autoinflammatory disease: biology, pathogenesis and therapeutic targeting. Nat Rev Rheumatol 18: 448-63

44. Fields JK, Kihn K, Birkedal GS, Klontz EH, Sjostrom K, et al., (2021) Molecular Basis of Selective Cytokine Signaling Inhibition by Antibodies Targeting a Shared Receptor. Front Immunol 12: 779100

45. Rydberg Millrud C, Deronic A, Gronberg C, Jaensson Gyllenback E, von Wachenfeldt K, et al., (2023) Blockade of IL-1alpha and IL-1beta signaling by the anti-IL1RAP antibody nadunolimab (CAN04) mediates synergistic anti-tumor efficacy with chemotherapy. Cancer Immunol Immunother 72: 667-78

46. Hojen JF, Kristensen MLV, McKee AS, Wade MT, Azam T, et al., (2019) IL-1R3 blockade broadly attenuates the functions of six members of the IL-1 family, revealing their contribution to models of disease. Nat Immunol 20: 1138-49.

47. Apte RN, Voronov E (2017) Immunotherapeutic approaches of IL-1 neutralization in the tumor microenvironment. J Leukoc Biol 102: 293-306

48. Du P, Xu L, Qiu W, Zeng D, Yue J, et al., (2015) A fully human monoclonal antibody with novel binding epitope and excellent neutralizing activity to multiple human IFN-alpha subtypes: A candidate therapy for systemic lupus ery-thematosus. MAbs 7: 969-80

## Supplementary Materials

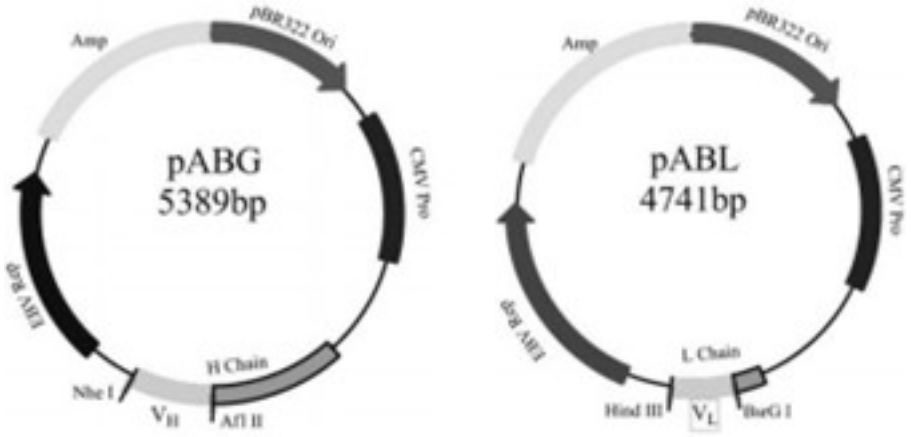


**Figure S1:** The schematic map of the recombinant plasmid. pABL is the λ light chain and pABG is the γ1 heavy chain. All were constructed by our laboratory.

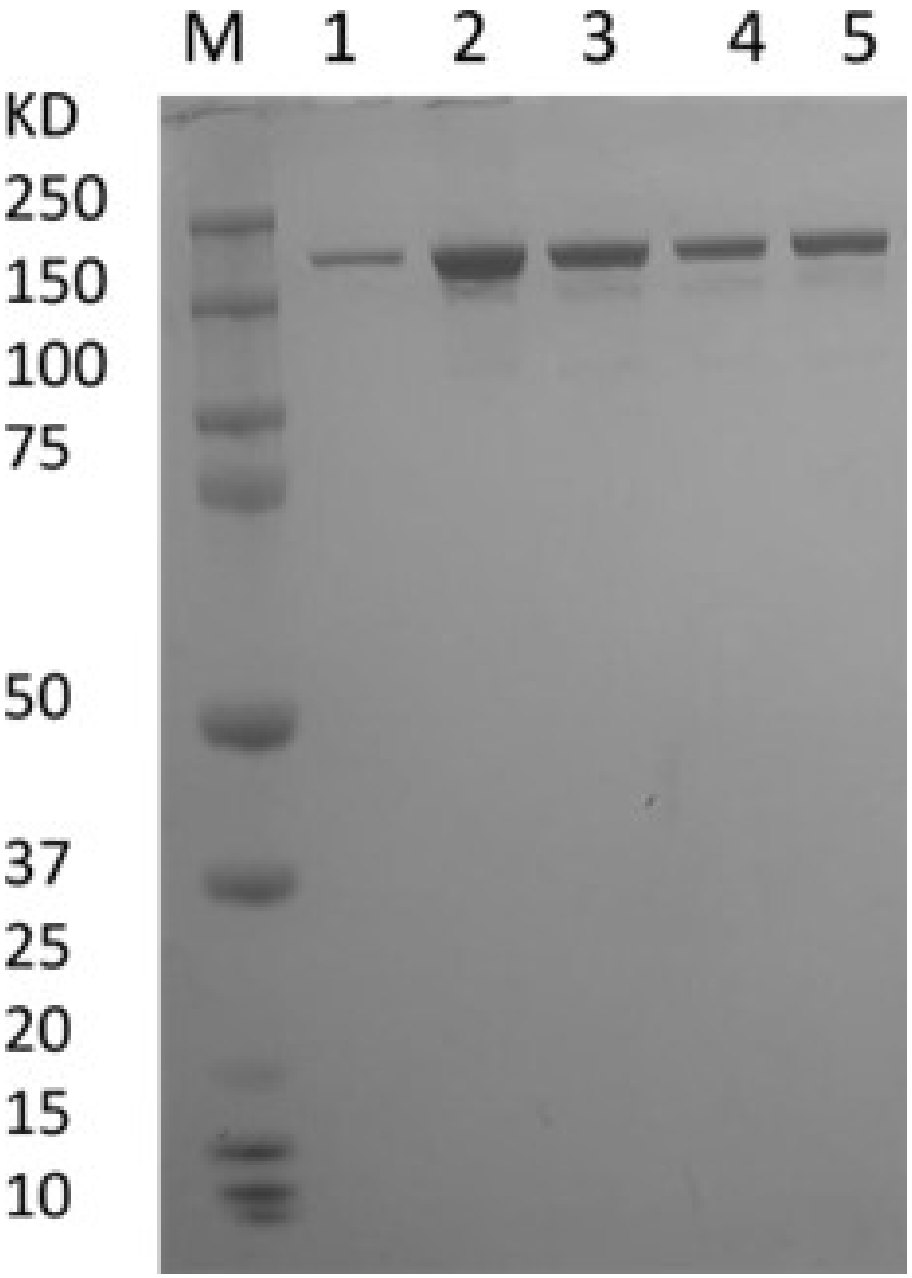

**Figure S2:** SDS-PAGE results of purified antibodies. Lanes 1-5 are AET1903, AET1904, AET1906, AET1907, and AET1912 antibodies, respectively, and show purified antibodies were non-reducing; M represents a standard protein marker. The protein band was clear, and the purity was high.

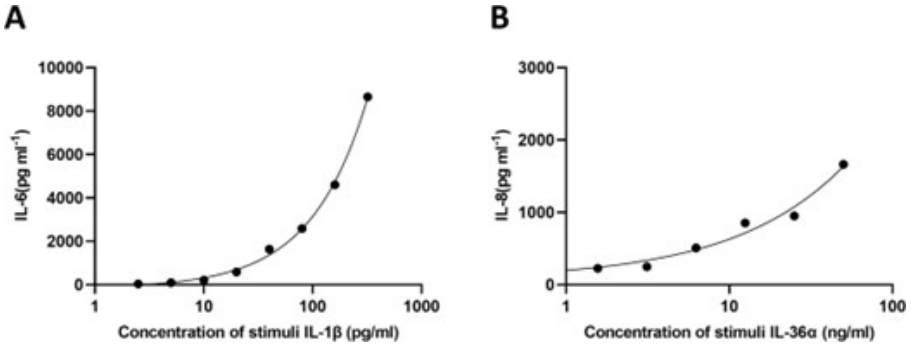


**Figure S3:** IL-1 family-mediated secretion of cellular inflammatory cytokines. (A) The effect of IL-1β at a concentration gradient of 2.5-320 pg/mL on the quantity of IL-6 secreted by A549 cells. (B) The effect of IL-36α at a concentration gradient of 0.78-50 ng/mL on the quantity of IL-8 secreted by HaCaT cells.

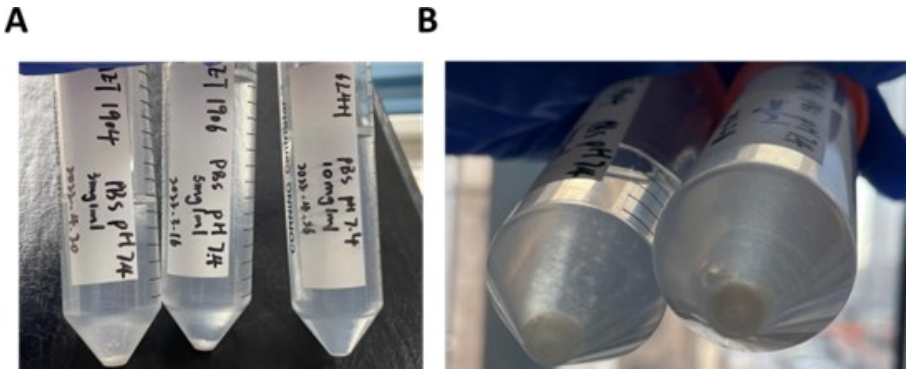


**Figure S4:** Improving solubility of re-paired antibody. Antibodies placed for several months were observed, and it was noted that AET1904 (3 mg/mL) and AET1906 (5 mg/mL) precipitated to varying degrees (two left tubes in A, and B), while the re-paired antibody 6L4H (10 mg/mL) remained homogeneous (far right in A). Taking 6L4H as an example, the name represents a new antibody obtained by combining the light chain (L) of AET1906 and the heavy chain (H) of AET1904.

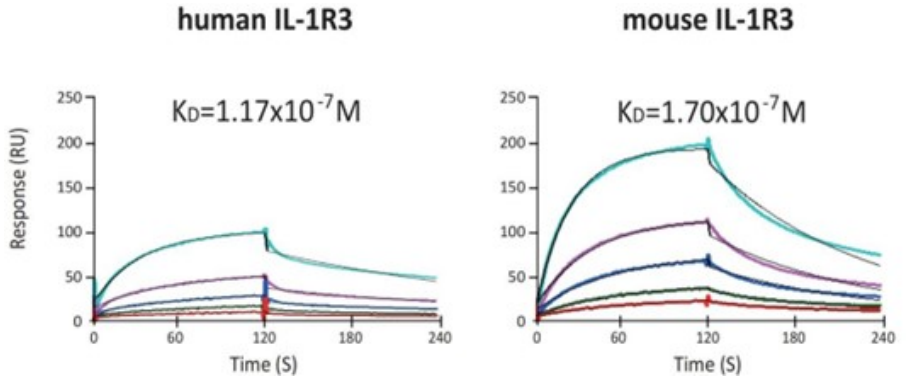


**Figure S5:** Representative sensorgrams of antibodies in SPR assays. Sensorgrams show the interaction between re-paired antibody 6L4H and

human IL-1R3-His (left panel) or mouse IL-1R3 (right panel) at a descending concentration range of 600 nM, 300 nM, 150 nM, 75 nM, 37.5 nM. The value is derived from the steady-state calculation (1:1 binding) for a better fit.

**Table S1:** Selection of anti-IL-1R3 mAbs from the sc-Fv library;

| Round | 1 | 2 | 3 | 4 | 5 |
|---|---|---|---|---|---|
| Type Conc.(μg/mL) × Vol. (mL) | human IL-1R3 | | mouse IL-1R3 | | |
| Coated | 20 × 1.0 | 10 × 1.0 | 3.0 × 1.0 | 1.3 × 1.0 | 1.0 × 1.0 |
| Input Phage (pfu)* | $2 \times 10^{9}$ | $1 \times 10^{10}$ | $6 \times 10^{10}$ | $1.2 \times 10^{11}$ | $8 \times 10^{11}$ |
| Binding Condition | | 4 °C, 18-20 h | 37 °C, ~1.2 h | 37 °C, ~1.2 h | 4 °C, >40 h |
| Initial Wash** (Times) | 10+15+0 | 10+15+8 | 0+20+10 | 23 + 30+8 | 12+6+15 |
| Extensive Washes*** | | | 10 min | | |
| Phage Recovered (pfu) | $2.0 \times 10^{4}$ | $2.9 \times 10^{5}$ | $3.6 \times 10^{5}$ | $3.0 \times 10^{4}$ | 5400 |
| Positive Clone (% | | | 58 | 15.63 | 34 |
| Specific Clone**** | | | 12 | 18 | 7 |

Antibodies were coated with human IL-1R3 and mouse IL-1R3 alternately. In each turn, the coating concentration was reduced, and the washing was increased. *Two different sublibraries of λ3H3 and λ3H5 were mixed for screening. **PBST = PBS containing 0.1% Tween 20. Each washing lasted for 5 min.

***Extensive washing (PBS containing 0.2 M NaCl) was performed by adding glycine-HCl (pH = 4.5) buffer for a 10 min incubation before discarding buffer. ****Screened target genes were cloned into human IgG1 expression vectors, and then expressed in the FreeStyle™ 293-F system.

**Table S2:** Thermostability results of antibodies;

| Sample | AET1903 | AET1904 | AET1906 | AET1907 | AET1912 |
|---|---|---|---|---|---|
| Tm(℃) | 70.34 | 70.2 | 71.47 | 67.915 | 69.05 |

In the high-throughput protein stability analysis system, the Tm & Tagg with optional DLS program is used, in which Tm is determined based on Tm-266 nm laser excitation protein endogenous fluorescence. Protein unfolding during the heating process leads to a fluorescence spectrum change, and conformational change is estimated by collecting full spectrum data and detecting spectrum change. In general, the higher the Tm value is, the greater the thermal stability.

**Table S3:** Binding activity of re-paired antibodies;

| EC50 (ng/mL) | | | EC50 (ng/mL) | | |
|---|---|---|---|---|---|
| Antibody | | | Antibody | | |
| | huIL-1R3 | moIL-1R3 | | huIL-1R3 | moIL-1R3 |
| 3H4L | # | 4 | 7H3L | NA | 3126 |
| 3H6L | 2369 | NA | 7H4L | ~124 | 503 |
| 3H7L | 3740 | 2856 | 7H6L | ~238 | 285 |
| 3H12L | / | / | 7H12L | 67 | 3 |
| 4H3L | 6555 | 91 | 12H3L | ~3621 | 11840 |
| 4H6L | 712 | 40 | 12H4L | ~1070 | 2282 |

| | | | | | |
|---|---|---|---|---|---|
| 4H7L | 6384 | 2354 | 12H6L | 4267 | 254 |
| 4H12L | 5452 | 443 | 12H7L | ~49 | NA |
| 6H3L | 1864 | 317 | 1903 | 1487 | 271 |
| 6H4L | / | / | 1904 | 793 | 14 |
| 6H7L | # | 621 | 1906 | 859 | 12 |
| 6H12L | 4370 | 14300 | 1907 | 11 | 1 |
| | | | 1912 | 16 | 34 |

Antibodies were coated with 1 μg/mL of human IL-1R3 or mouse IL-1R3 in 96-well plates; then, antibodies of 0.0045 μg/mL to 10 μg/mL were diluted in a concentration gradient. NA represents no detectable binding activity; "~" represents approximately equal to. "/" means no purified sample was obtained. Taking 6L4H as an example, the name represents a new antibody obtained by combining the light chain (L) of AET1906 and the heavy chain (H) of AET1904. EC50 values were measured by GraphPad Prism Software 9.0.

**Table S4:** Kinetic parameters of re-paired antibodies interacting with human IL-1R3 and mouse IL-1R3.

| **Abs** | **Antigen** | **ka (104M-1s-1)** | **kd (10-3s-1)** | **KD (10-7M)** | **χ2 (RU²)** |
|---|---|---|---|---|---|
| 6L4H | huIL-1R3 | 4.22 | 4.95 | 1.17 | 6.36 |
| | moIL-1R3 | 5.42 | 9.19 | 1.7 | 3.25 |

ka, association rate constant; kd, disassociation rate constant; KD, equilibrium disassociation constant; KD=kd/ka. χ2 is the chi-square value between the fitted curves and response curves. The value is derived from the steady-state calculation (1:1 binding) for a better fit.